Journal of Statistical Physics, Vol. 107, Nos. 3/4, May 2002 (© 2002)

Coherent Stochastic Resonance in One Dimensional Diffusion with One Reflecting and One Absorbing Boundaries

Asish K. Dhara[1, 2] **and Tapan Mukhopadhyay**[1]

Received May 21, 2001; accepted November 28, 2001

It is shown that the single-step periodic signal (periodic telegraph signal) can not produce coherent stochastic resonance for diffusion on a segment with one absorbing and one reflecting end points while the multi-step periodic signal does. The general features of this process are exihibited. The resonant frequency is found to decrease and the mean first passage time at resonant frequency increases linearly, as we increase the length of the medium. The cycle variable is shown to be the proper argument to express the first passage probability at resonance. A formula for first passage probability at resonance is derived in terms of two universal functions, which clearly isolates its dependence on the length of the medium.

KEY WORDS: Coherent stochastic resonance; first passage probability.

1. INTRODUCTION

After the pioneering achievement of separation of large DNA molecules in gel medium by the application of uniform and time-dependent periodic electric field,[1, 2] the mechanism of cooperative interplay between random noise and a deterministic periodic signal attracts considerable interests. It has been found that with this technique, large molecules in the size range 2 to 400 kb exihibit size-dependent mobilities. Similar ideas have also arisen in other types of chromatographic processes.[3]

The mean first passage time (MFPT) is a useful tool to investigate the diffusive transport property in a medium. The theory of first passage time has been worked out in great detail for both infinite medium and explicitly

[1] Variable Energy Cyclotron Centre, 1/AF Bidhan Nagar, Calcutta-700064, India.
[2] To whom correspondence should be addressed; e-mail: akd@veccal.ernet.in

0022-4715/02/0500-0685/0

time-independent diffusive processes.[4–6] However, for explicitly time-dependent processes and in finite medium analytic closed form expressions are not available. In this respect also this problem attracts much attentions to the scientific community.

The first analysis of this phenomena has been done for a random walk on a lattice numerically, and for a diffusive process in a continuous medium with periodic signal of small amplitude perturbatively.[7] Their results indicate that the oscillating field can create a form of coherent motion capable of reducing the first passage time by a significant amount. This enhancement of the mobility of a particle in a diffusive medium by the application of proper oscillating field is known in the literatures[8, 9] as coherent stochastic resonance (CSR).

In order to investigate the reason for this cooperative behavior of random noise and deterministic periodic signal this problem has been formulated in much simpler terms by approximating the sinusoidal periodic signal by the telegraph signal[8] and subsequently it has been shown[9, 10] that the telegraph signal can not produce CSR. Finally, when the sinusoidal signal has been approximated as a multi-step periodic signal,[10] the non-monotonic behavior of mean first passage time (MFPT) with respect to the characteristic frequency of the periodic signal is recovered explaining the reason of CSR in the case of two absorbing boundaries explicitly. The general characteristics of the moments of first passage time probability density function (referred to shortly as "first passage probability" (FPP) hereafter) in their calculations[10] for continuous medium and with arbitrary amplitide of the periodic signal are found to be in agreement with the numerical simulation of the random walk model on a lattice.[7]

When the phenomenon of CSR is being discussed for the linear systems, it turns out that the boundary conditions play a crucial role in some models.[11–14] Doering and Gadoua have considered the jumps in a linear double-well potential when the potential fluctuates between two values at a rate γ. The non-monotonic dependence of the MFPT on γ (called "the resonance activation") has been found to occur when one of the boundaries is absorbing and the other is reflecting.[11] Brey and Cassado-Pascual[12] have investigated random walk on a one dimensional lattice in which at any time each site has one of two transition rates which are being allowed to change at random times. Similar effects of boundary conditions have been observed. Linear models with asymmetric[13] and symmetric[14] random telegraph signals (dichotomous noise) also show that MFPT behaves non-monotonically with the jump rates for the transition between these two states when one of the boundaries is absorbing and the other is reflecting.

In this paper we consider an overdamped linear system driven by a sinusoidal force and embedded in a noisy environment which is taken to be

Gaussian white. As mentioned before, no analytic closed form expression is available in the literature for this explicitly time dependent problem. We therefore approximate the sinusoidal force (signal) by a multi-step periodic signal (explained below). This is the system which we considered before.[10] The only difference is that in this paper we have asymmetric boundary conditions, i.e., one end point is a reflecting boundary and the other one is absorbing while in the previous work[10] both the boundaries were taken as absorbing.

We note that the linear system with single-step periodic signal (periodic telegraph signal) could be recovered as a special case of this system with multi-step periodic signal. The linear system with single-step periodic signal (periodic telegraph signal) with one reflecting and one absorbing boundaries has been considered in the literature.[14] Non-monotonic behavior of MFPT with respect to the characteristic frequency of the periodic telegraph signal has been reported.[14] In this paper we show that the telegraph signal does not produce any non-monotonic behavior of MFPT with respect to frequency. This result is in direct contradiction with the result obtained in ref. 14. The explanation of this contradiction is stated in the text below (in Section 2 and Section 3.1).

The paper is organised as follows. In Section 2, we give the formulation of the problem. The basic structure of this formulation is similar as before.[10] The only change with the previous one is to incorporate the effect of asymmetric boundary conditions. The results of the calculations are discussed in Section 3. First we present the general characteristics of CSR. The calculation clearly exhibits how resonance appears in our multi-step approximation and fails to show in single-step telegraph approximation of the periodic signal. The general characteristics of the moments and the characteristic features of FPP for this phenomena are also presented in this subsection. In the next subsection we focus on the resonance point and demonstrate some special features associated with it. In particular, we show in this subsection (Section 3.2) that the cycle variable is the proper argument to express the FPP at resonance. Further, it is shown that the FPP at resonance can be expressed in terms of two universal functions. This feature clearly isolates its dependence on the length of the medium. Finally, few concluding remarks have been added in Section 4.

2. FORMULATION OF THE PROBLEM

We consider diffusion in one dimension perturbed by a periodic force. The motion of the particle is given by the Langevin equation

$$\dot{X} = A \sin \Omega t + \xi(t) \tag{1}$$

where X refers to the stochastic variable, A and Ω are the amplitude and frequency of the sinusoidal signal and $\xi(t)$ is a zero mean Gaussian white noise of strength D with auto-correlation function given by

$$\langle \xi(t)\, \xi(t') \rangle = 2D\delta(t-t') \tag{2}$$

The motion is confined between a reflecting boundary at $x=0$ and an absorbing boundary at $x=L$. The Fokker–Planck equation corresponding to Eq. (1) is

$$\frac{\partial p(x,t)}{\partial t} = -\frac{\partial j(x,t)}{\partial x} = -A \sin \Omega t \frac{\partial p(x,t)}{\partial x} + D \frac{\partial^2 p(x,t)}{\partial x^2} \tag{3}$$

where $p(x,t)$ and $j(x,t)$ refer to the probability density and probability current density respectively at position x and at time t. The reflecting boundary condition at $x=0$ implies that $j(0,t)=0$ and absorbing boundary conditions at $x=L$ suggests that $p(L,t)=0$. We now introduce the dimensionless variables

$$\xi = (A/D)\, x, \qquad \theta = (A^2/D)\, t, \qquad \omega = \Omega/(A^2/D) \tag{4}$$

to write Eq. (3) in terms of new variables:

$$\frac{\partial p(\xi,\theta)}{\partial \theta} = -\sin \omega\theta \frac{\partial p(\xi,\theta)}{\partial \xi} + \frac{\partial^2 p(\xi,\theta)}{\partial \xi^2} \tag{5}$$

The boundary conditions are rewritten as $j(0,\theta) = p(\Lambda,\theta) = 0$, where $\Lambda = (A/D)\, L$.

No analytic solution exists for Eq. (5) with the boundary conditions mentioned. We thus introduce a scheme to approximate the force $\sin \omega\theta$ as a multi-step periodic signal.[10] This scheme is in contrast to the procedure adopted in ref. 7, where they discretise the Eq. (3) using finite difference method and simulate the problem on a lattice of space and time. The construction of multi-step periodic signal is available in ref. 10 and shown in Fig. 1. The specific feature of the construction is that in order to reach the maximum value $(=1)$ of the signal from the zero level we have to have $(p+1)$ steps up and from the maximum to the zero level we have $(p+1)$ steps down. The construction clearly shows that we get back the usual telegraph signal with $p=0$. Approximation of the sinusoidal signal by the usual telegraph signal has been made by ref. 8 in the case of two absorbing boundaries.

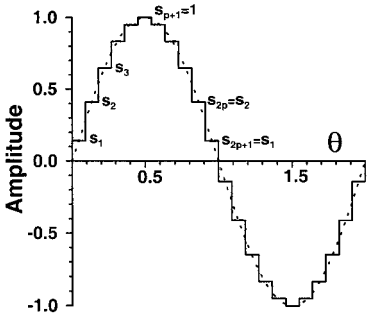

Fig. 1. Sinusoidal signal (dashed curve) and approximated six-step ($p = 5$) periodic signal (solid curve) for the full one cycle as a function of θ.

The Fokker–Planck equation [Eq. (5)] in each interval with this scheme will be that for a constant bias, namely

$$\frac{\partial p(\xi, \theta)}{\partial \theta} = \frac{\partial U'(\xi)\, p(\xi, \theta)}{\partial \xi} + \frac{\partial^2 p(\xi, \theta)}{\partial \xi^2} \tag{6}$$

where $U'(\xi) = -s(s > 0)$ for the positive half cycle and equals to $+s(s > 0)$ for the negative half cycle with s being the value of s_k[10] for the corresponding time interval (see Fig. 1). We wish to express the conditional probability density in each interval in terms of complete set of normalised eigenfunctions satisfying the boundary conditions mentioned above. For that it is convenient to cast Eq. (6) into an eigenvalue problem of Schrödinger type by setting

$$p(\xi, \theta) = e^{-\lambda\theta} e^{\pm s\xi/2} \phi(\xi) \tag{7}$$

Substituting the ansatz Eq. (7) in Eq. (6) we obtain

$$\lambda = \mu^2 + s^2/4 \tag{8}$$

$$\phi'' + \mu^2 \phi = 0 \tag{9}$$

Reflecting boundary condition at $\xi = 0$, $j(0, \theta) = 0$, and absorbing boundary condition at $\xi = \Lambda$, $p(\Lambda, \theta) = 0$, associated with Eq. (6) with the help of Eq. (7) take the following form

$$[\tfrac{1}{2} U'\phi + \phi']_{\xi=0} = 0, \qquad \phi(\Lambda) = 0 \tag{10}$$

In the future development we associate the index n for the positive half-cycle and index m for the negative.

Employing these boundary conditions [Eq. (10)] in some interval in the positive half-cycle, the normalised eigenfunctions, $\phi_n(\xi)$ are obtained as

$$\phi_n(\xi) = \left[\frac{2}{\Lambda - \dfrac{\sin 2\mu_n \Lambda}{2\mu_n}} \right]^{1/2} \sin \mu_n(\Lambda - \xi) \tag{11}$$

where μ_n are obtained by solving the transcendental equation

$$\sin \mu_n \Lambda + \frac{2\mu_n}{s} \cos \mu_n \Lambda = 0 \tag{12}$$

The corresponding eigenvalues λ_n are given by

$$\lambda_n = \mu_n^2 + s^2/4 \tag{13}$$

We note that λ in Eq. (7) must be positive. Therefore in the range $-s^2/4 < \mu^2 < 0$, employing the above procedure one obtains the eigenfunction $\phi(\xi) \sim \sinh \kappa(\xi - \Lambda)$, where κ would be obtained as a solution of the transcendental equation

$$s\Lambda \sinh \kappa\Lambda + 2\kappa\Lambda \cosh \kappa\Lambda = 0 \tag{14}$$

where $\kappa^2 = -\mu^2$, $\kappa > 0$. As no solution exists for Eq. (14), we say that for the positive half-cycle the normalised eigenfunctions $\phi_n(\xi)$ in Eq. (11) form a complete set. On the other hand, for the negative half-cycle, employing the similar procedure we find the normalised eigenfunctions $\phi_m(\xi)$ and the transcendental equations associated with them are similar as in Eqs. (11)–(12) with suffix n replaced by m for $\mu_m \neq 0$. For $\mu_m = 0$, boundary conditions suggest that one nontrivial eigenfunction exists only when $s\Lambda = 2$. Thus if the value of Λ is such that $s\Lambda = 2$, apart from the eigenfunctions as stated above, one more eigenfunction exists which is

$$\phi_{\mu_m = 0}(\xi) = \left(\frac{3}{\Lambda^3} \right)^{1/2} (\xi - \Lambda) \tag{15}$$

Further, in the range $-s^2/4 < \mu^2 < 0$, only one nontrivial eigenfunction exists for $s\Lambda > 2$. This is given by

$$\phi_\kappa(\xi) = \left[\frac{2}{\dfrac{\sinh 2\kappa\Lambda}{2\kappa} - \Lambda} \right]^{1/2} \sinh \kappa(\Lambda - \xi) \tag{16}$$

where $\kappa^2 = -\mu^2$, $\kappa > 0$ and it is obtained by solving the transcendental equation

$$-\sinh \kappa \Lambda + \frac{2\kappa}{s} \cosh \kappa \Lambda = 0 \tag{17}$$

while in the range $0 < s\,\Lambda < 2$, no nontrivial eigenfunction exists. The corresponding eigenvalues in all the cases are given by

$$\lambda_m = \mu_m^2 + s^2/4 \tag{18}$$

For a given value of Λ, the corresponding set of $\{\phi_n(\xi)\}$ forms the complete set of eigenfunctions in the positive half-cycle while the set $\{\phi_m(\xi)\}$ [including Eq. (16) or Eq. (15) as the case may be] forms the complete set in the negative half-cycle.

Once the complete set of normalised eigenfunctions and eigenvalues are determined the conditional probability density function $p(\xi, \theta \mid \xi', \theta')$ in the positive half-cycle could be expressed as

$$p(\xi, \theta \mid \xi', \theta') = \sum_n u_n^+(\xi)\, u_n^-(\xi') \exp[-\lambda_n(\theta - \theta')] \tag{19}$$

where

$$u_n^{\pm}(\xi) = \exp(\pm s\xi/2)\, \phi_n(\xi) \tag{20}$$

with s as the value of s_k in the corresponding subinterval of the multi-step signal[10] where the conditional probability is being decomposed and $\phi_n(\xi)$ and λ_n are given by Eqs. (11) and (13) respectively. The conditional probability density function in any interval, say l, can then be calculated from the previous history by convoluting it in each previous intervals.[10]

For the negative half-cycle the calculation of conditional probability density function is similar except that we have to replace the index n by m and the conditional probability density function is decomposed as

$$p(\xi, \theta \mid \xi', \theta') = \sum_m u_m^-(\xi)\, u_m^+(\xi') \exp[-\lambda_m(\theta - \theta')] \tag{21}$$

where the expressions for $u_m^{\pm}(\xi)$ are same as in Eq. (20) with n replaced by m and λ_m are given by Eq. (18).

The survival probability at time θ when the particle is known to start from $\xi = \xi_0$ at $\theta = 0$ is defined as

$$S(\theta \mid \xi_0) = \int_0^{\Lambda} d\xi\, p(\xi, \theta \mid \xi_0, 0) \tag{22}$$

The first passage probability (FPP) $g(\theta)$ is defined as

$$g(\theta \mid \xi_0) = -\frac{dS(\theta \mid \xi_0)}{d\theta} \tag{23}$$

Physically, $g(\theta)\, d\theta$ gives the probability that the particle arrives at the absorbing boundary in the time interval θ and $\theta + d\theta$. From this density function one can calculate various moments:

$$\langle \theta^j \rangle = \int_0^\infty d\theta\, \theta^j g(\theta) \tag{24}$$

From Eq. (24) one can easily calculate mean first passage time (MFPT) $\langle \theta \rangle$ and the variance $\sigma^2 = \langle \theta^2 \rangle - \langle \theta \rangle^2$ of the density function $g(\theta)$.

As stated in the introduction, the present formulation is similar to that of our earlier work for the case of two absorbing boundaries.[10] Of course, the nature of the eigenfunctions and the associated eigenvalues are different due to changed boundary conditions in two different cases.The survival probabilities in the ith cycle and kth subinterval of positive and negative half cycle of the multi-step periodic signal are given below.

$$\begin{aligned} S(\theta \mid \xi_0) &= \sum_n C^+_{n,k} \exp[-\lambda_{n,k}(\theta - 2(i-1)\triangle\theta)]\, O_{n,k}, \\ &\qquad \text{in the positive half cycle} \\ &= \sum_m C^-_{m,k} \exp[-\lambda_{m,k}(\theta - (2i-1)\triangle\theta)]\, E_{m,k}, \\ &\qquad \text{in the negative half cycle} \end{aligned} \tag{25}$$

where $k = 1, 2, \ldots, N(=2p+1)$ and

$$C^+_{n,k} = \int_0^\Lambda d\xi\, u^+_{n,k}(\xi) \tag{26a}$$

$$C^-_{m,k} = \int_0^\Lambda d\xi\, u^-_{m,k}(\xi) \tag{26b}$$

and the functions $O_{n,k}$, $E_{m,k}$ are generated through the recursion relations:

$$O_{n,1} = F_{i-1,n} \tag{27a}$$

$$O_{n,k} = \sum_{n'} \langle u^-_{n,k} \mid u^+_{n',k-1} \rangle \exp[(k-1)(\lambda_{n,k} - \lambda_{n',k-1})\,\tau]\, O_{n',k-1} \tag{27b}$$

$$E_{m,1} = \sum_{n} \langle u^{+}_{m,1} \mid u^{+}_{n,N} \rangle \exp[-\triangle\theta\lambda_{n,N}]\, O_{n,N} \tag{27c}$$

$$E_{m,k} = \sum_{m'} \langle u^{+}_{m,k} \mid u^{-}_{m',k-1} \rangle \exp[(k-1)(\lambda_{m,k} - \lambda_{m',k-1})\,\tau]\, E_{m',k-1} \tag{27d}$$

$$F_{i,n} = \sum_{m} \langle u^{-}_{n,1} \mid u^{-}_{m,N} \rangle \exp[-\triangle\theta\lambda_{m,N}]\, E_{m,N} \tag{27e}$$

with $k = 2, 3, \ldots, N$, half period $\triangle\theta = \pi/\omega$, subinterval width $\tau = \frac{\triangle\theta}{2p+1}$ and $F_{0,n} = u^{-}_{n,1}(\xi_0)$. The angular bracket in any equation implies dot product of the corresponding functions, for e.g.,

$$\langle u^{+} \mid u^{-} \rangle = \int_0^{\Lambda} d\xi\, u^{+}(\xi)\, u^{-}(\xi) \tag{28}$$

The cycle variable i runs over positive integers; i.e., $i = 1, 2, 3, \ldots$. As the quantities are different for different subintervals specified by k, the double subscripts are used in order to specify to which specific subinterval they refer. Note that in many earlier equations, for e.g., in Eqs. (11)–(13), Eqs. (18)–(21) only one subscript and in Eq. (28) no subscript are used for brevity though they are double subscripted quantities through the value of s_k. The effect of history is explicit in the expressions for survival probabilities. Once the survival probability $S(\theta \mid \xi_0)$ is obtained from these formluae, the FPP, MFPT and the corresponding variance are obtained by employing Eqs. (23)–(24). Evaluation of MFPT and other relevant quantities requires sum of infinite series which must be truncated in order to obtain a final result. Convergence of MFPT is ensured by gradually increasing the number of terms (i.e., number of eigenvalues) for the calculation. The process is truncated when MFPT does not change upto two decimal point of accuracy with the change of number of terms.

3. RESULTS AND DISCUSSIONS

The survival probability, mean first passage time (MFPT), corresponding variances and first passage probability (FPP) are calculated using the derived formulae for this process. The results are summarised below.

3.1. General Features of CSR

The MFPT is calculated for single-step telegraph signal ($p = 0$) with $\xi_0 = \Lambda/2$. Most of the calculations are done with this specific value of ξ_0. The variation of the results with variation of ξ_0 is also demonstrated [see

the text below]. No nonmonotonous behavior is observed in MFPT as we vary the frequency ω. This is in disagreement with Gitterman's observation.[14] Because of the wrong set of eigenvalues and corresponding eigenfunctions in both positive and negative half-cycles used to express the conditional probability density, Gitterman observed nonmonotonic dependence of MFPT with respect to the characteristic frequency of the periodic telegraph signal.

The calculation is done for the length $\Lambda = 20$ and the result is shown in the curve (a) of Fig. 2. However, when we take $p = 1$, i.e., when the sinusoidal signal is approximated by two-step periodic signal, the calculation of MFPT for the same length shows clearly the nonmonotonous behavior. This is shown in curve (b) of the same figure. This is therefore the first stage where resonance appears when passing from telegraph ($p = 0$) to sinusoidal ($p = \infty$) signal. It is worth to mention that similar situation is observed[10] in the case of two absorbing boundaries. This result clearly demonstrates that mere flipping of the bias (signal) direction periodically would not produce the coherent motion. As the rate of flipping increases it merely prevents the particle more to reach the absorbing boundary and therefore MFPT increases monotonically. It may be noted that when the flipping rate is very high, the effect of signal is almost nil and the transport is effectively diffusive in nature. This is of course true in any type of periodic signal. Therefore, for any type of approximation of the sinusoidal signal or for any value of p, this feature would show up. In particular, for $p = 1$, we observe from curve (b) of Fig. 2 that MFPT would asymptotically reach the diffusive limit $3\Lambda^2/8$ (= 150 in this case). The usual telegraph signal

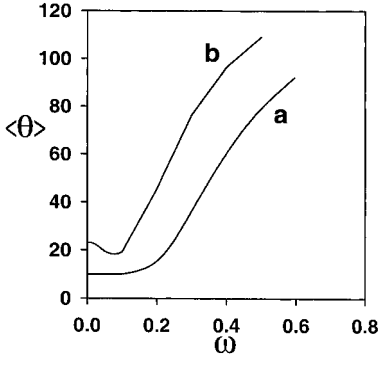

Fig. 2. MFPT $\langle\theta\rangle$ as a function of ω; (a) for p = 0; the usual telegraph signal. This curve is monotonously increasing with frequency showing no resonance, (b) for p = 1; the two-step periodic signal, [$\Lambda = 20$, $\xi_0 = \Lambda/2$]. (The variables and parameters used in all the figures are all dimensionless).

offers a constant bias of maximum magnitude for the larger time than for a two-step approximation. Hence the particle always has a larger probability of reaching the absorbing boundary in short time for $p=0$ case than for $p>0$ case. Hence MFPT for $p=0$ and for any ω is always less than for $p>0$ case. This is observed in Fig. 2.

In CSR we always have a competition between diffusion and oscillatory effect of the bias. For very large frequency as the bias effect becomes ineffective MFPT would essentially be guided by diffusive process. For zero frequency of the multi-step periodic signal the MFPT can be analytically evaluated. When it starts from the mid-point of the medium it expresses as

$$\langle\theta(\omega=0,\xi_0=\Lambda/2)\rangle=0.5(\Lambda/s_1)-\left(\frac{2e^{-3s_1\Lambda/4}}{s_1^2}\right)\sinh(s_1\Lambda/4) \tag{29}$$

When frequency of the multi-step periodic signal is very small, the process is predominantly diffusion with constant value of the bias, $s_1=0.5\sin(\frac{\pi}{2p+1})$ effective for $0<\theta\leqslant\frac{\pi}{\omega(2p+1)}$. As the frequency ω is very small, this small bias s_1 is active for most of the time. However, as frequency increases slowly, the increased bias forces $s_1, s_2,\ldots$ apart from s_1 ($s_1<s_2, s_3,\ldots$) would be operative. These increased biased values reduce the survival probability and also MFPT. But when the frequency becomes very high, oscillatory effect of the signal makes the effect of the signal insignificant and MFPT would be more. Thus non-monotonocity appears in MFPT as a function of frequency. For $p=1$ approximation of sinusoidal signal we observe the non-monotonocity of MFPT . On the other hand, for usual telegraph signal ($p=0$ case), for very low frequency, from the very beginning bias force affects the particle with its maximum strength ($s_1=1$). When the frequency is very low, this constant bias diffusion continues for a longer time and there is no change-over of the magnitude of the bias as in the case of $p=1$. After having a flip, the particle again suffers a constant bias diffusion in the direction opposite to the previous one and towards the reflecting boundary. As frequency increases slowly, this picture remains unchanged until a stage reaches for which the flipping effect becomes dominant during the particle's survivality inside the medium and MFPT increases. This is observed in Fig. 2.

Next we continue all our calculation with $p=5$ or, with six-step telegraph signal. Calculation reveals that the value of MFPT does not change much from that with $p=1$. On the other hand, $p=5$ signal approximates the sinusidal signal better than $p=1$ signal. We restrict our calculation with $p=5$ approximation of the periodic signal.

We calculate the MFPT $\langle\theta\rangle$ and the variance σ^2 as a function of frequency ω for different lengths ($\Lambda=10, 20, 30, 40, 50$). Both the cumulants

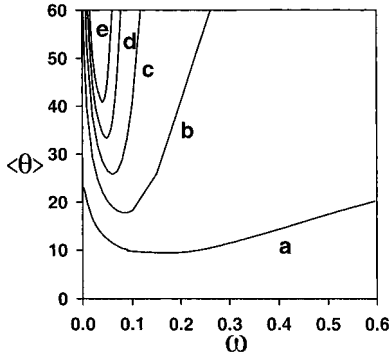

Fig. 3. MFPT $\langle\theta(\omega)\rangle$ as a function of frequency ω; (a) $\Lambda = 10$, (b) $\Lambda = 20$, (c) $\Lambda = 30$, (d) $\Lambda = 40$, (e) $\Lambda = 50$, $[p = 5, \xi_0 = \Lambda/2]$.

go through a minimum as frequency rises from very low value for each length Λ. It is observed that the minimum for both the moments occur almost at the same frequency for each length. This shows that the maximum cooperation between the deterministic signal and random noise occurs at this resonant frequency. The value of MFPT $\langle\theta\rangle$ increases with the length at all frequencies. This is understandable because as length increases, on an average the particle will spend more time in the medium before reaching the absorbing boundary. It is also observed that the frequency at which the minimum occurs shift towards low frequency as the length increases. The behavior of MFPT as a function of frequency for different lengths is presented in Fig. 3.

The lowering of the dispersion at resonant frequencies confirms that the cooperation is maximum at these frequencies. Dispersion is more for higher lengths and merges to a specific value at very low frequency at various lengths.

All the previous calculations are done when the particle starts initially from the mid point of the medium, i.e., ξ_0 in Eq. (22) is taken as $\Lambda/2$. At the length $\Lambda = 30$ the resonant frequency is found to be 0.06. The calculations are done one at resonant frequency and other two at the off-resonant frequencies ($\omega = 0.1$ and $\omega = 0.0$) when the particle starts from $\xi_0 = \beta\Lambda$ where β lies between 0 and 1. For zero frequency the MFPT can be analytically obtained. Its expression reads as

$$\langle\theta(\omega = 0, \beta\Lambda)\rangle = \frac{\Lambda(1-\beta)}{s_1} - \left(\frac{2e^{-s_1\Lambda(1+\beta)/2}}{s_1^2}\right)\sinh(s_1\Lambda(1-\beta)/2) \quad (30)$$

The curves are shown in Fig. 4. It is evident that the value of $\langle\theta\rangle$ is less for resonant frequency (curve (a)) than for its value for off-resonant frequencies (curves (b) and (c)). For each curve the maximum value of $\langle\theta\rangle$ occurs at lower values of β or, when the particle starts from the left of the interval (near the reflecting boundary). Our signal starts with positive half-cycle and therefore the survival time of the particle would be more if the particle starts from the left of the interval. On the other hand, if it starts from right half of the medium (near the absorbing boundary), the initial surge of the signal helps the particle to reach the absorbing boundary more quickly. Hence average time of duration decreases. For curve (b) where the frequency of the signal ($\omega = 0.1$) is more than the resonant frequency, the oscillatory contribution is more than that for the resonant frequency making the MFPT large than for curve (a). For curve (c) where the frequency is zero ($\omega = 0.0$), the particle experiences a constant bias ($s = s_1$) towards the absorbing boundary all the time. This is in contrast to the other two cases where the particle has a probability to experience bias of magnitude more than s_1. As the value of s_1 (the first value of six-step periodic signal) is smallest hence the curve (c) lies always above the curves (a) or (b).

The FPP $g(\theta; \omega)$ for different frequencies are calculated and plotted as a function of θ for a given length $\Lambda = 30$ [Fig. 5]. One can clearly see the evolution of the FPP profile as the frequency increases from $\omega = 0.0$ to $\omega = 0.1$.

At very small frequency , the particle is acted on by a constant force $s = s_1$ (in the multistep periodic approximation) almost all the time before it reaches the absorbing boundary. The FPP curve shows that we have only one maximum in the entire θ-range.

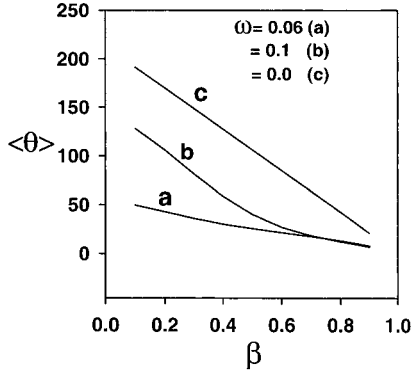

Fig. 4. MFPT $\langle\theta\rangle$ as a function of β for length $\Lambda = 30$; (a) for resonant frequency $\omega^* = 0.06$, (b) for off-resonant frequncy $\omega = 0.1$, (c) for off-resonant frequncy $\omega = 0.0$, [$p = 5$].

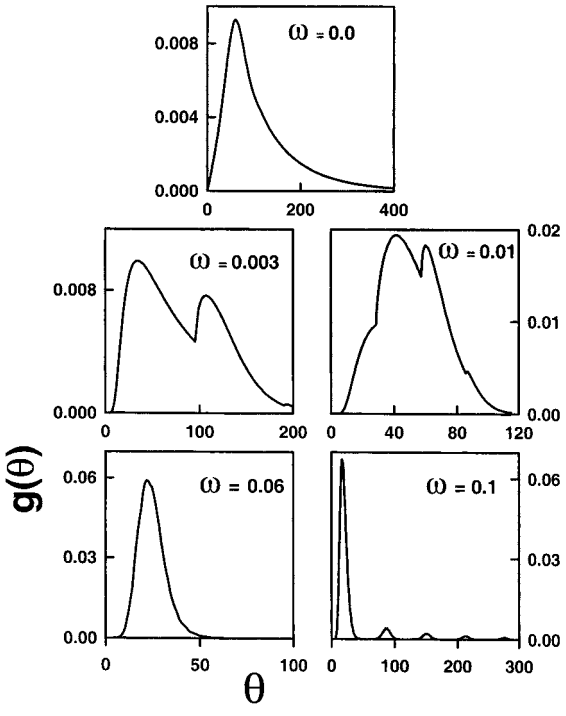

Fig. 5. FPP $g(\theta)$ as a function of θ for $\Lambda = 30$ for frequencies $\omega = 0.0$, 0.003, 0.01 (before resonance), $\omega = 0.06$ (resonant), $\omega = 0.1$ (after resonance) respectively, $[p = 5, \xi_0 = \Lambda/2]$.

As the frequency slowly increases, one finds that, apart from only one maximum (like the one at very small frequency) other small peaks at larger θ also show up gradually. Also, these new small peaks start becoming stronger as the frequency increases. This is because the particle which initially sees a constant bias ($s = s_1$) for some time encounters an increased bias after a while (larger θ) and so on before reaching the absorbing boundary. As $\int g(\theta)\, d\theta = 1$, the area under the major profile decreases and is compensated by extra peaks at higher θ. We therefore see that as the frequency increases continuously, the small peaks that show up at higher θ start growing and at the same time the first peak slowly decreases keeping the total area same.

The resonance occurs at $\omega = 0.06$ for $\Lambda = 30$. The MFPT has a minimum at that frequency. It has been argued that the synchronization between the signal and the noise is maximum at this frequency causing the enhancement of the probability of reaching the absorbing boundary at a short time. The FPP profile at resonance (at this frequency) evidently

shows a dominant single peak. We also see that the constituent profiles of FPP adjust themselves in a very distinct way, as the frequency increases, in order to produce a dominant maximum at the resonance.

Beyond the resonance (at higher frequencies) the peaks are quite numerous, distinct and identified separately, while the area of the dominant peak (at resonance) starts decreasing. In other words, the degree of synchronization is getting reduced as we go beyond the resonant frequency—if we identify the area of the peaks as the degree of synchronization (considering total area is normalized).

3.2. Special Features at Resonance

In this subsection we concentrate on the behaviour of the system at the resonance point. We have already discussed some general characteristics of CSR in the previous subsection. We find that for each length, Λ, a corresponding frequency ω^* exists for which $\langle\theta\rangle$ and σ^2 become minimum implying that the maximum cooperation between the deterministic periodic signal and random noise of the environment is taking place in helping the particle to reach the absorbing boundary. One therefore would naturally inquire about the relation of ω^* with Λ. In the range of Λ we studied, this curve is very well fitted with the formula

$$\omega^* = C/\Lambda^{\gamma} \tag{31}$$

where $C = 0.8053$, and $\gamma = 0.7615$.

The values of MFPT at resonance $\langle\theta(\omega^*)\rangle$ is found to increase linearly with the length Λ and within the range of Λ we consider the relation between them is fitted to

$$\langle\theta(\omega^*)\rangle = 0.79\Lambda + 1.85 \tag{32}$$

Of course, there will be deviation from this linear behaviour as Λ decreases further because $\langle\theta\rangle$ can not become positive for $\Lambda = 0$ (corresponding to $L = 0$); $\langle\theta\rangle$ should be zero at $\Lambda = 0$.

We have already seen that at the resonance frequency we have single dominant peak of FPP, $g(\theta)$ [Fig. 5]. Since it is a general feature, for each length Λ we should get such behaviour. When we plot $g(\theta)/\omega^*$ as a function of $[\omega^*(\Lambda)\,\theta]$, we find that the curves for different lengths superpose over each other [Fig. 6] and the pattern of $g(\theta)/\omega^*$ for different Λ or ω^* is very similar, i.e., at particular values of $[\omega^*\theta]$, all curves show their maxima, and change in the behavioral patterns of the curves occur exactly at the same places of $[\omega^*\theta]$. This shows that $[\omega^*\theta]$ or the cycle number is the correct variable to describe the resonance behaviour. We may further

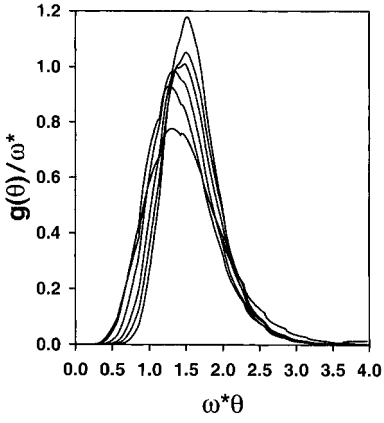

Fig. 6. The dominant peaks of $g(\theta)/\omega^*$ at resonant frequencies for different lengths ($\Lambda = 20$, 25, 30, 35, 40, 50) as a function of $\omega^*\theta$. The lowermost curve is for $\Lambda = 20$, and as length increases gradually upper curves are generated, $[p = 5, \xi_0 = \Lambda/2]$.

note that such scaling of FPP would not be possible for any frequency other than the resonant frequencies because any frequency which is not the resonant frequency for one length may turn out to be the resonant frequency for some other length and the features of FPP are different for resonant and off-resonant frequencies as has been observed from Fig. 5. The major dominant peaks of FPP $g(\theta)/\omega^*$ for different lengths ($\Lambda = 20$, 25, 30, 35, 40, 50) are drawn as a function of $[\omega^*\theta]$ in Fig. 6. The lowermost curve is for $\Lambda = 20$ and as length increases the upper curves are generated. The peaks for all the curves occur nearly at a quarter of a cycle.

Having found the proper scaling of the argument of FPP, it is natural to enquire whether the FPP, $f \equiv g(\theta)/\omega^*$ can also be scaled properly, so that once $f(x)$ with $x = \omega^*\theta$ is found for one length, the function $f(x)$ can be obtained for any arbitrary length.

In order to investigate this issue, first we observe that going from $f(x; \Lambda_1)$ to $f(x; \Lambda_2)$, where Λ_1 and Λ_2 are two different lengths we have to multiply one function by different amount depending on the value of the argument. Thus if at all any scaling relation exists, this should be of the form

$$f_{\mu\Lambda}(x) = f_{\Lambda}(x)\, \mu^{\alpha(x)} \tag{33}$$

Note that Eq. (33) is a hunch and it is indeed found to be true with $\alpha(x)$ given in Fig. 7. We note that $\alpha(x)$ is universal and it decreases very rapidly to large negative values for very low x. We thus have two types of scaling on FPP at resonance. One is on its argument, namely $\theta \rightarrow (\omega^*\theta)$

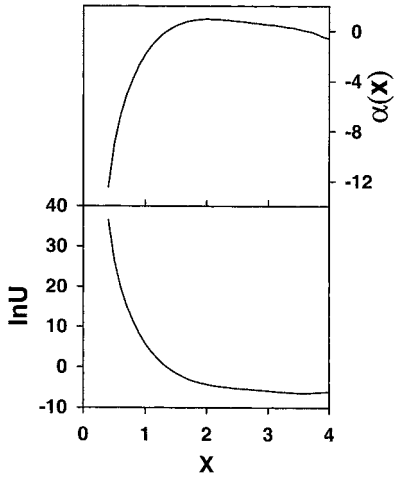

Fig. 7. The universal functions $\alpha(x)$, $\ln U(x)$ as a function of x.

and the other is on the function itself through the universal function $\alpha(x)$. From the relation (33) it is obvious that

$$\Lambda^{-\alpha(x)} f_\Lambda(x) = [\mu\Lambda]^{-\alpha(x)} f_{\mu\Lambda}(x) \tag{34}$$

The Eq. (34) shows that the function $\Lambda^{-\alpha(x)} f_\Lambda(x)$ is independent of Λ and it is again universal. We verify this result in our calculation of FPP for different lengths and call this function $U(x)$. The $\ln U(x)$ is also plotted in Fig. 7. Note that $\ln U(x)$ takes a very large positive values for low x in order to have finite but small value of $f_\Lambda(x)$ in that region. At $x \simeq 1.5$ where the peak of $f_\Lambda(x)$ occurs, $\ln U(x)$ is small negative while $\alpha(x)$ takes small positive value. Thus we could express $f_\Lambda(x)$ at resonance in terms of two universal functions $U(x)$ and $\alpha(x)$ as

$$f_\Lambda(x) = U(x)\, \Lambda^{\alpha(x)} \tag{35}$$

The expression (35) clearly isolates the dependence of FPP on length of the medium Λ at resonance. The form (35) for $f_\Lambda(x)$ is plotted for a typical length $\Lambda = 30$ and compared with values calculated from Eq. (23) in Fig. 8. It is giving an excellent agreement. Further with this form, the MFPT is found for different Λ. It also yields required behaviour as in Eq. (32). This shows that not only we have found a scaling behaviour given by Eq. (33) which takes $f(x)$ from one length to the other, it is also possible to obtain a simple expression Eq. (35) for $f_\Lambda(x)$ for any arbitrary length.

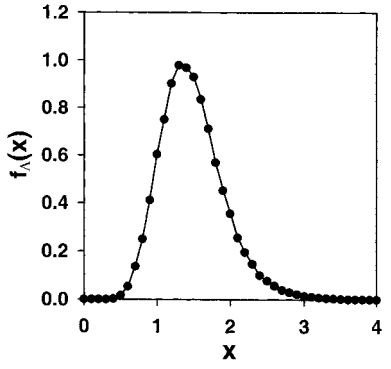

Fig. 8. $f_\Lambda(x)$ as a function of x for $\Lambda = 30$ at resonance from values calculated from Eq. (23) (filled circle) [$p = 5, \xi_0 = \Lambda/2$] and $f_\Lambda(x)$ according to the formula (35) as a function of x for $\Lambda = 30$ (solid curve).

4. CONCLUDING REMARKS

We consider a diffusive transport process perturbed by a sinusoidal signal in continuous one dimensional medium having one reflecting and one absorbing boundaries. We showed explicitly that the cooperative behaviour between the deterministic periodic signal and random noise leading to coherent motion occurs when the time-dependent sinusoidal signal is approximated by a multistep periodic signal and not with single-step telegraph signal.

Although we study the process with $p = 5$ periodic signal, the formulation is quite general and applicable for any approximation with arbitrary number of steps. This formulation can also be applied to any arbitrary continuous periodic signal. Further, no perturbation of the signal amplitude is assumed in this formulation.

It is observed that in the low time regime frequency dependent bias force (i.e., the chance of having increased values of the bias in the same direction is more for relatively high frequency than for low frequency) has the key factor for resonance to occur. For very high frequency the bias effect is practically absent and the motion is purely diffusive in nature. At the resonance the maximum cooperation between the noise and the periodic signal takes place making the MFPT a minimum.

The resonant frequency decreases and the mean first passage time at resonant frequency increases linearly, as we increase the length of the medium. The corresponding relations are obtained. This fact provides a measure of the time scale of this process at resonance.

Other important characteristic that we observe is that at the resonance the FPP for various lengths have similar behaviour if we scale the argument of FPP as $\theta \rightarrow (\omega^* \theta)$. The curve shows that there is single dominant peak, which is a reflection of the fact that the synchronization between the deterministic periodic signal and the random noise is maximum at resonance. The peak positions of these curves occur very near to a quarter of a cycle showing that the cycle number is the correct argument to describe FPP at resonance.

We also show that there exists a scaling relation between FPP at various lengths through some universal function $\alpha(x)$. The exact expression for FPP at resonance is obtained in terms of two universal functions, which clearly isolates its dependence on the length of the medium. This is a special feature of coherent stochastic resonance. This form may be of use in obtaining quicker result in cases where more complex situation is called for.

All calculations are made to an end when the survival probability takes a value 1×10^{-3}. We observe that if we cut off the calculations for more lower values of survival probability it does not affect MFPT but the variances are slightly affected.

From Fig. 6 we observe a slight deviation of the peak positions but we believe that if the sinusoidal signal is approximated by more than a $p = 5$ periodic signal the position of all the peaks will be the same.

REFERENCES

1. D. C. Schwartz and C. R. Cantor, *Cell* **37**:67 (1984).
2. G. F. Carle, M. Frank, and M. V. Olson, *Science* **232**:65 (1986).
3. I. J. Lin and L. Benguigi, *Sep. Sci. Tech.* **20**:359 (1985).
4. G. H. Weiss, *Adv. Chem. Phys.* **13**:1 (1967).
5. C. W. Gardiner, *A handbook of Stochastic Methods*, 2nd ed. (Springer-Verlag, New York, 1985).
6. N. G. van Kampen, *Stochastic Processes in Physics and Chemistry* (North-Holland, Amsterdam, 1991).
7. J. E. Fletcher, S. Havlin, and G. H. Weiss, *J. Statist. Phys.* **51**:215 (1988).
8. J. Masoliver, A. Robinson, and G. H. Weiss, *Phys. Rev. E* **51**:4021 (1995).
9. J. M. Porra, *Phys. Rev. E* **55**:6533 (1997).
10. Asish K. Dhara and Tapan Mukhopadhyay, *Phys. Rev. E***60**:2727 (1999).
11. C. R. Doering and J. C. Gadoua, *Phys. Rev. Lett.* **69**:2318 (1992).
12. J. J. Brey and J. Cassado-Pascual, *Physica A* **212**:123 (1994).
13. M. Gitterman, R. I. Shrager, and G. H. Weiss, *Phys. Rev. E* **56**:3713 (1997).
14. M. Gitterman, *Phys. Rev. E* **61**:4726 (2000).